Academic Journal of Science and Technology
ISSN: 2771-3032 | Vol. 16, No. 3, 2025

In Vitro Study of Nasal Spray Deposition Patterns Based on Eight Realistic Nasal Cavity Models

Hongxian Ren

Atsenbo Pharmaceutical Technology Co., Ltd, Suzhou, 215151, PR China

Abstract: To systematically evaluate the effects of different nasal sprays on the deposition of nasal turbinate, nasal septum and olfactory region in different populations. This study utilized CT scanning technology and reverse engineering techniques to create eight realistic 3D nasal models. The effects of particle size and plume angle on different nasal (gender and age) depositions were studied. The significance of differences in particle deposition across different individuals and devices in various regions of the nasal cavity was explored. The results showed that the deposition efficiency of all four devices was above 80%, with plume angles between 25° and 34.3°. The Device D was more likely to reach the olfactory. The deposition in the nasal septum was not affected by individual differences. There is a positive correlation between the nasal cavity size and age, and their relationship follows a linear regression equation: $y = 65.11 + 0.65x$. However, the growth rate of the olfactory region's size slows down with increasing age, and its proportion decreases. An increase in the plume angle will result in a more uniform deposition distribution. Smaller particles are more easily delivered to the posterior regions of the nasal cavity. Differences in age and gender have an obvious impact on the deposition distribution in the nasal septum and nasal turbinate regions, with older individuals and males exhibiting more favorable deposition patterns in these areas. This advantage becomes more pronounced with age. The drug is more likely to reach the posterior nasal cavity in children.

Keywords: Deposition patterns; nasal spray; gender and age; particle size; plume angle.

1. Introduction

Nasal drug delivery is a promising method of drug administration that can be used for both local delivery and systemic treatment through rapid absorption, thus attracting widespread attention [1-3]. In addition to avoiding the first-pass effect when the drug is taken orally, this method also offers a high bioavailability. It can not only treat respiratory diseases such as congestion and allergies but also be used to deliver locally acting medications for treating rhinitis and sinusitis. Additionally, it enhances the speed and extent of blood absorption and boosts immune responses to vaccines in a non-invasive manner [4-6].

Due to the higher research and development potential of nasal administration, more academic and industrial teams have been stimulated to conduct research[7, 8].However, the anatomy of the nasal cavity is extremely complex. The region in the anterior part of the nasal cavity is called the nasal vestibule. This area is covered with squamous epithelial cells and contains nasal hairs and secretory glands that restrict drug penetration into the tissues, thus, this area is not typically regarded as a site of drug absorption [9]. So in order to increase the efficiency of nasal drug delivery, drug deposition in the nasal vestibule should be avoided. Instead, the drug should be delivered to specific target sites. These targets are mainly located in the nasal passages and turbinate regions of the central and posterior nasal cavity [2, 10]. On the one hand, the nasal turbinate region is highly vascularized, with a rich network of blood vessels and extensive surface mucosa. Additionally, the convoluted structure of this area significantly increases the surface area of the nasal cavity, thereby providing a larger region for drug absorption. Drugs can be absorbed through the nasal mucosa into the systemic circulation, allowing for the treatment of systemic diseases [11, 12]. On the other hand, the olfactory region located at the tip of the nasal cavity is the only part of the human central nervous system (CNS) that is in direct contact with the environment[13]. Its surface is covered with olfactory epithelium consisting of microvilli cells, supporting cells, olfactory cells, and basal cells[14]. Therefore, drugs deposited in the olfactory region can be rapidly transferred to the CNS, bypassing the complex multicellular structure of the blood-brain barrier, to treat CNS diseases[15-19]. However, delivery of drugs to these targets is challenging[20]. Due to the triangular valve area located at the posterior part of the nasal vestibule, approximately 2-3 cm from the nasal entrance, which has the smallest cross-sectional area, it acts as a flow-limiting region before expanding into the main nasal passage[21]. This presents an obstacle to effectively delivering drugs into the main nasal passage, resulting in the majority of drug particles being deposited in the anterior third of the nasal cavity[2, 22-26]. At the same time, it is also important to prevent smaller particles from entering the deeper regions of the respiratory system, as this could not only waste the medication dose and fail to achieve the desired therapeutic effect, but also pose risks of respiratory irritation and decreased lung function [27, 28].

Various nasal drug delivery devices such as nasal drops, pressurized metered-dose inhalers, liquid sprays and dry powder formulations are currently in use[3, 20]. Liquid formulations dominate the drug market due to their portability and the added benefit of humidification, which helps alleviate the dryness and crusting commonly associated with nasal diseases[29, 30]. As a first-line treatment, doctors often recommend nasal sprays to their patients[31, 32]. The particle size of liquid formulations used for nasal drug delivery is typically larger than 10μm. These particles are expelled from the spray device through the nozzle at a very high velocity[33]. Meanwhile, the inhaled airflow through the nasal cavity can increase the emission velocity of the particles, helping to promote the deposition of liquid spray formulations[34, 35]. To deliver sufficient drug particles to the target site, multiple

factors need to be considered, such as the drug formulation, delivery method, spray atomization, spray device, and patient handling[6, 36-39]. Among these, the interaction between the spray device and the drug formulation generates a spray plume with unique geometry and characteristics, which markedly impacts the deposition pattern of particles in the nasal cavity[40]. Therefore, assessing the various spray characteristics and user-related factors associated with the spray device itself is crucial for understanding drug particle deposition and optimizing device design[28, 41].

Although local deposition of nasal drugs is best characterized through in vivo clinical trials using radiolabeled drug formulations, these studies are both expensive and time-consuming. Moreover, the results obtained are often qualitative, providing only semi-quantitative data[10, 42]. In vitro methods can effectively avoid the issues mentioned above and help optimize the factors influencing regional deposition under controlled conditions, allowing for the refinement of both the device and formulation [2, 10, 42]. FOO et al. used MRI derived nasal replicas to measure deposition patterns of solutions with a wide range of surface tension and viscosity. The results showed that sprays with smaller plume angles were able to reach the nasal turbinate region with deposition efficiencies approaching 90%. Meanwhile, the effects of particle size, viscosity, and inhalation flow rate on particle deposition in the nasal turbinate were not significant. Instead, the plume angle and delivery angle were identified as key factors determining deposition efficiency[42]. Guo et al. studied the impact of device structural parameters and formulation physical properties on the performance of nasal spray delivery. The results indicated that the device driving speed and gelling agent concentration had a significant effect on the deposition efficiency, whereas the surfactant concentration had almost no effect on the properties of the nasal sprays[43]. Cheng et al. evaluated four nasal spray pumps and found that the plume angle and particle size distribution were important factors in deposition[44]. Most of the previous studies were conducted based on adult models. Since children's nasal valves are narrower than those of adults, airflow velocities in the nasal valve region is higher in children, and anterior deposition of nasal sprays may be increased compared to that of adults[45]. Sawant et al. used nasal casts obtained from MRI-based images of 12-year-old children to test the deposition patterns of nasal sprays in children. It was found that only a small amount of the spray reached the nasal turbinate. The differences in deposition patterns of nasal sprays between adults and children may result in varying therapeutic outcomes for these two populations[28]. Inthavong et al. proposed that the design of nasal spray devices should aim to reduce the inertia of particles to penetrate the nasal valve region effectively. Additionally, they emphasized the need to find a method that ensures the deposition of the drug within the nasal passages without allowing it to escape into the lungs[41]. To address this, some researchers have proposed a breath-driven bidirectional drug delivery method. Compared to spray pumps, this novel breath-driven bidirectional device provides greater deposition in clinically significant areas beyond the nasal valve, significantly reducing drug deposition in the nasal vestibule[5, 46].

Current nasal spray devices are widely used, but continuous exploration and improvement are necessary to ensure higher drug delivery efficiency. The study of drug particle deposition in specific regions of the nasal cavity is of great significance as each disease corresponds to a different potential target site. In this paper, eight subject nasal cavity models were reconstructed taking into account the effect of individual differences in users (gender and age). Four commercially available nasal spray devices were analyzed using statistical experiments to investigate particle size, plume angle and individual differences on nasal deposition. The results of the study can provide help and guidance for the design and optimization of nasal spray devices.

2. Materials and Methods

2.1. Nasal Airway

Computed tomography (CT) scans of the nasal cavity of eight Asian volunteers (two adult males, two adult females, two boys, and two girls) were performed with the approval of the Institutional Review Board of the Second Affiliated Hospital of Xi'an Jiaotong University. The information of the scanned images was exported and the exported files were saved in DICOM format. The images were processed and optimized using Mimics and 3DSlicer, and subsequently the 2D images were converted into 3D solid models, which were exported in S Tereo Lithography (STL) format. The model was also refined and segmented on ANSYS Spaceclaim and Solidworks. The physiological and health information of the volunteers is shown in Table I, and symbols are used instead of names to protect the privacy of the volunteers.

Table I. Physical and health information of volunteers

Name	Age	Gender	Group	Health
CF1	4	female	children	Adenoid hypertrophy
CF2	6	female	children	Adenoid hypertrophy
CM1	4	male	children	Adenoid hypertrophy
CM2	5	male	children	Adenoid hypertrophy
AF1	22	female	adult	health
AF2	39	female	adult	Chronic sinusitis, inferior turbinate hypertrophy
AM1	45	male	adult	Chronic sinusitis, bilateral maxillary sinus window surgery
AM2	31	male	adult	Chronic sinusitis, Bilateral complete sinusotomy.

The nasal cavity model in STL format was imported into the geometric modeling software for segmentation. Since the anatomy of the nasal cavity is a complex and specialized field, and the difficulty lies in the difficulty of defining the boundaries of the segmented regions, the segmentation of the nasal cavity model in this paper was carried out under the professional guidance of an Otolaryngologist.

The final model was made using the photosensitive resin material UV Curable Resin on a ZhongRui SLA660 printer with a print thickness of 0.1mm.

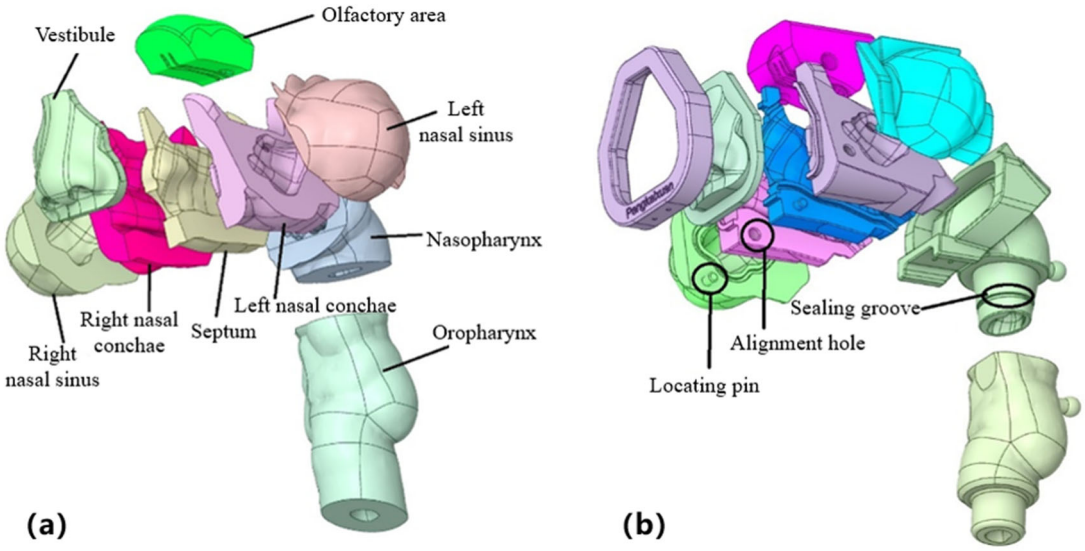

Figure 1. Schematic of the solid model of the nasal cavity, (a) Segmentation region, (b) Post-processing.

As shown in Fig. 1(a), the nasal cavity model was structurally and anatomically segmented into nine parts, including nasal vestibule, left sinus, right sinus, left turbinate, right turbinate, nasal septum, olfactory region, nasopharynx, and oropharynx, taking into account the different regions of the nasal cavity disease foci. The segmented parts need to be fully assembled and airtight to ensure proper functionality. As shown in Fig. 1(b), axial pins and sealing grooves were added between adjacent parts, and sealing strips were placed between parts to prevent gas leakage. Finally, the post-processed nasal cavity model is connected using a fastening method. The method chosen in this chapter is the latch fastening, which is a quick-release fastening connection. Since it only requires a single hand to flip the latch, it can be quickly opened or closed within one or two seconds, making it more convenient and efficient. The reconstructed physical model of the nasal cavity is shown in Fig. 2.

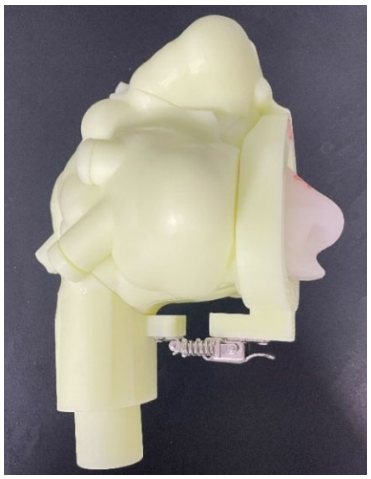

Figure 2. Assembly of the solid model of the nasal cavity.

2.2. Spraying Devices and Formulations

Figure 3. Four commercially available liquid nasal sprays.

Four commercially available liquid nasal sprays commonly used in otolaryngology were provided by a practicing otolaryngology clinician as shown in Fig. 3, and the relevant parameters are shown in Table II. Device A: Mometasone Furoate Nasal Spray (also known as NASONEX), manufactured by MSD Belgium BVBA, is indicated for the prevention and treatment of nasal disorders such as seasonal or perennial rhinitis sinusitis in adults, adolescents, and children between the ages of 3 and 11. Device B: Fluticasone Furoate Nasal Spray, manufactured by GlaxoSmithKline (UK) Ltd, is mainly used for the treatment of nasal congestion, runny nose, sneezing and other symptoms caused by allergic rhinitis. Device C: Fluticasone propionate nasal spray, also manufactured by GlaxoSmithKline (UK) Ltd, for the prevention and treatment of seasonal allergic rhinitis and perennial allergic rhinitis. And Device D: XHANCE Nasal Spray (OptiNose US, Inc.), which also has fluticasone propionate as its main ingredient, differs from Device C in

that it employs a bi-directional delivery method and is primarily used for the treatment of chronic sinusitis with nasal polyps in adult patients 18 years of age or older.

Table II. Parameters associated with the four nasal sprays

Device	Company	Dose	Formula
Device A	MSD Belgium BVBA	140 sprays	Mometasone furoate 50μg/spray
Device B	GlaxoSmithKline	120 sprays	Fluticasone furoate 27.5μg/spray
Device C	GlaxoSmithKline	120 sprays	Fluticasone propionate 50μg/spray
Device D	OptiNose	120 sprays	Fluticasone propionate 93μg/spray

Numerous studies have shown that the primary deposition mechanism of nasal sprays is inertial impaction, which can be controlled by varying the spray parameters of the spray device[6, 37, 47]. The spray parameters include the following: particle size, spray plume angle, insertion angle and particle release position[48]. Therefore, it is particularly crucial to measure for the above spray parameters.

2.3. Particle Size Distribution Measurement

The laser particle size tester used in this paper is the HELOS | SPRAYER with ROTOR system from Sympatec, Germany. The particle size test range is 0.25-875μm, and the accuracy of multiple sampling test is <0.3%. Before each experiment, a test was initiated by shaking the nasal spray vigorously and pressing the spray button continuously until uniform particles appeared. After the completion of each test, wipe the residual particles from the spray nozzle with a dust-free cloth and proceed to the next test. At the end of each nasal spray test, the test program should be updated and the next round of testing should follow.

According to the FDA guidance, studies should be conducted within a range of 2 to 7 cm from the spray nozzle. Therefore, this study selected two testing points at distances of 3 cm and 6 cm from the nozzle. The characteristic values D10, D50, and D90 represent the particle sizes below which 10%, 50% (the volume median), and 90% of the particle volume are found, respectively. The coefficient of variation (COV) of the test results should be satisfied: the COV of D50 of the test group is ≤10%, and the COV of D10 and D90 are both ≤15%. To ensure the reproducibility of the experiment in accordance with national standards, each nasal spray was tested 6 times per group. The results of each group were evaluated based on the COV, and the conformity of the test results was determined accordingly [6].

2.4. Spray Plume Angle Measurement

The plume angle is the angle formed between the conical region ejected from the nozzle and the apex of the nozzle end. For nasal sprays, FDA guidelines recommend using a non-collision method to measure plume geometry[40].

In this study, the SprayVIEW test system was used to measure the plume angle, and the relevant parameters are shown in Table III. Before starting, calibrate the force and displacement sensors of the auto-trigger to ensure precise control of the stroke and drive force during auto-triggering. For each nasal spray, on first use, the nasal spray was shaken vigorously and the spray button was pressed continuously until uniform particles appeared. Each nasal spray was tested individually for five consecutive times, with the spray particles filtered out by the exhaust air of the environmental shield between each test and left to stand for 30 s.

Table III. Relevant parameters of the test system

parameters	specification
Trigger Type	SprayVIEW NSP
Trigger Mode	Automatic characterization at runtime
driving force	57.036N
Trigger speed	90mm/s
Trigger acceleration	6000mm/s2
gas evacuation time	45s
settling time	30s
Test Distance from Nozzle	6cm

2.5. Nasal Spray Deposition Measurements

Kolor Kut /KK01 water test paste is an easy way to test for the presence of water. When the paste is applied to a surface, it changes color upon contact with water, shifting from light pink to purple-red. This color change provides a quick and easy visual indication of moisture. The MettlerToledo/MS204TS02 analytical balance is a precision electronic balance manufactured by Mettler-Toledo with a maximum weighing capacity of 220g and a readable accuracy of 0.1mg. The fixing bracket is a customized processing of a fixed adjustable angle device, can fix the nasal cavity model, and at the same time adjust the angle of the nasal spray inserted into the nostrils. Mitutoyo/500-152-30 is a digital vernier caliper produced by Mitutoyo in Japan, the measuring range is 0-200mm, accuracy: ± 0.02mm.

To address the issue of abnormal data in deposition tests, the number of repetitions is set to three, and the COV of the deposition data is limited to 25%. When the COV of the sedimentary data was found to exceed 25%, additional test results were added to replace the original anomalous data[49].

The experimental procedure was as follows: firstly, the nasal model was disassembled, the KK01 water test paste was evenly applied to the inner surface of the nasal septum, sinuses and olfactory region. Each part of the nasal cavity model and the nasal spray are initially weighed and recorded. The nasal cavity model is then reassembled and fixed on the spray test platform. The nasal spray is inserted into the left nostril, and its angle is adjusted. The nasal spray is locked in place, and a manual trigger is used to activate the spray. After the test, any liquid particles remaining on the nozzle are

wiped off with a dust-free cloth. The nasal cavity model is disassembled again, and each part along with the nasal spray is weighed and recorded. Additionally, the length of any part that has changed color is measured, specifically the distance from the colored end to the end of the nasal cavity. The spray weight was obtained by the weight difference of the nasal spray before and after spraying. The weight difference of each component of the nasal cavity model before and after spraying provides the deposition amount for that specific area.

2.6. Statistical Analysis

The plume angles produced by the different nasal spray devices were evaluated using mean values and relative standard deviations. Due to the large number of samples, the deposition fraction in different regions were studied using mean values. The particle size distribution was expressed as mean± standard deviation. The Kolmogorov-Smirnov test and the Shapiro-Wilk test methods were used to test the normality of continuous variables in multiple independent groups. Continuous variables of multiple independent groups that follow a normal distribution are presented as mean ± standard deviation, while those that follow a non-normal distribution are presented as median (interquartile range). A p-value less than 0.05 was considered statistically significant.

3. Results

3.1. Particle Size Distribution

The compliant test data were extracted and organized while comparing the particle size distribution parameters of different nasal sprays as shown in Table IV. The volume median droplet size (D50) for devices A, B, C and D were 35.54±0.43, 72.45±0.78, 40.62±0.40 and 37.44±0.58 in the test point of 3 cm, respectively. At the 6 cm test point, D50 decreased by 17%-27%. Moving from the test point of 3 cm to the test point of 6 cm, the D10 value of the particle increased by 5.9% to 18.1%. The D50 of Device A increased by 5.5%, while the D50 of the other three nasal sprays decreased by 1.5% to 6.1%. The D90 value decreased by 3.8% to 10.2%. Additionally, as the test point changed, the D10 value of Device D showed the smallest change, only 5.9%, while the D10 value of Device A showed the largest change, reaching 18.1%. Among them, Device D exhibited the most stable particle size, while Device A showed the greatest variation in particle size with changes in the test points. The particle size of Device B is larger than that of the other three nasal spray products, nearly twice as large.

Table IV. Parameters of particle size distribution of different nasal sprays

Device	Test point /cm	$D_{10} \pm \sigma$/μm	$D_{50} \pm \sigma$/μm	$D_{90} \pm \sigma$/μm
Device A	3	14.66±0.41	35.54±0.43	79.16±0.50
Device B	3	29.00±0.80	72.45±0.78	130.10±1.76
Device C	3	15.57±0.47	40.62±0.40	98.63±1.75
Device D	3	15.61±0.26	37.44±0.58	82.60±1.14
Device A	6	17.32±0.77	37.49±0.70	71.84±1.91
Device B	6	32.49±0.89	68.65±1.19	125.21±1.15
Device C	6	17.17±0.39	38.16±0.83	89.88±2.87
Device D	6	16.53±0.81	36.89±0.66	74.20±1.05

3.2. Measurement of Plume Angle

The specific results are shown in Table V. From the table, it can be observed that Device D has the widest plume angle at 34.3±0.9°, while Device C has the narrowest at 25.0±0.7°, with statistically significant differences among the devices. The plume width follows a similar trend to the plume angle.

Table V. Plume Angle and Plume Width Results for Four Spray Devices

Device	Plume angle/°	Average plume width /mm
Device A	29.0±1.1	31.2±1.2
Device B	26.7±0.5	28.5±0.6
Device C	25.0±0.7	26.5±0.7
Device D	34.3±0.9	37.0±1.0

3.3. Differences in Nasal Airways

The dimensions of each partition of the nasal model of the eight volunteers in the depth direction of the nasal cavity (the nasal tract dimensions are the sum of the nasal vestibule and septum dimensions) are shown in Table VI.

Table VI. Dimensions of each partition of the nasal models in the direction of nasal depth (mm)

Name	vestibule	Septum	Left nasal concha	Right nasal concha	Olfactory region	Nasal airway
CF1	18.2	45.0	45.0	45.0	22.0	63.2
CF2	17.0	57.6	57.6	57.6	31.0	74.6
CM1	18.4	42.0	42.0	42.0	34.0	60.4
CM2	21.0	52.5	52.5	52.5	35.4	73.5
AF1	24.7	57.0	57.0	57.0	31.7	81.7
AF2	22.8	63.5	63.5	63.5	37.0	86.3
AM1	34.4	60.6	60.6	60.6	35.5	95.0
AM2	27.2	61.0	61.0	61.0	36.4	88.2

From Table VI, it can be concluded that adults have larger dimensions in all subdivisions of the nasal cavity than children, with the largest proportionate difference in the size of the nasal vestibule of 46.2%, while the smallest proportionate difference in the size of the olfactory region is only about 14.9%, and the difference in the entire nasal tract is about 29.3%.

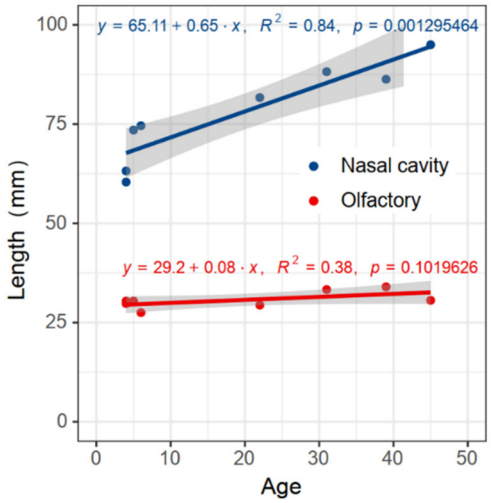

Figure 4. Four commercially available liquid nasal sprays.

The nasal cavity and olfactory region dimensions (y) of 8 patients were fitted with age (x) using linear regression equations. From the Fig. 4, it can be observed that the nasal cavity dimensions are positively correlated with age. As age increases, the dimensions of the nasal cavity in the depth direction continuously increase. However, the dimensions of the olfactory region do not show obvious changes with age.

3.4. Deposition Distribution by Device

As shown in Fig. 5, the mass deposition distribution of four devices in the nasal cavities of different populations is illustrated. For Device A, approximately 80% of the particles are deposited in the effective area. Nearly half of these particles end up in the nasal septum, one-third in the turbinate area, and almost none in the olfactory region. The particle amounts in the nasal vestibule and those remaining on the nozzle are generally less than 10%. However, for adult males, only about 70% of the particles are deposited in the effective area. For AM1, around half of the particles are deposited in the nasal septum, 15% in the nasal vestibule, and over 10% remain on the nozzle. For AM2, only about 40% of the particles are deposited in the nasal septum, about 15% in the turbinate area. Interestingly, approximately 10% of the particles are found in the olfactory region, which is unique among the eight nasal cavity models, being the only one with olfactory region deposition.

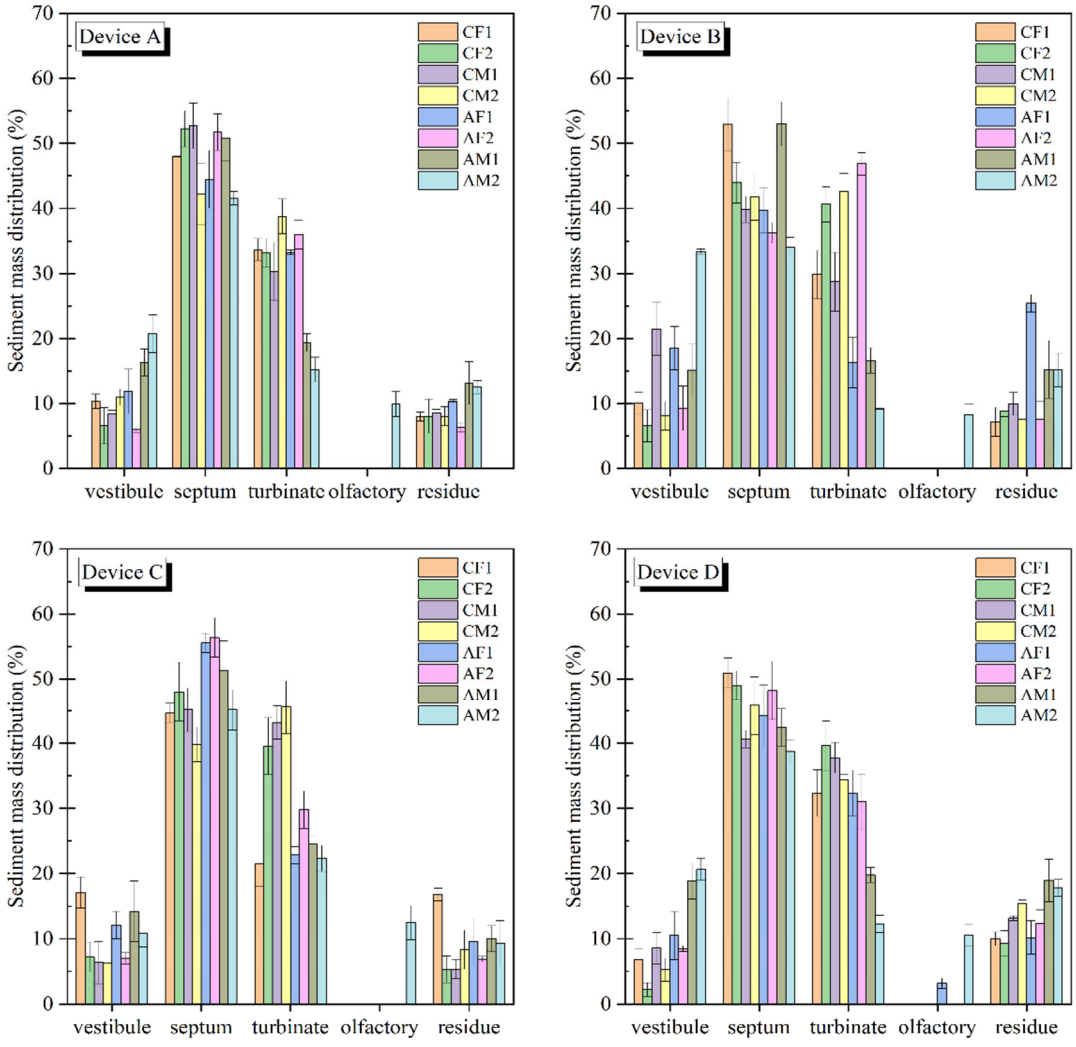

Figure 5. Mass deposition distribution of four devices in the nasal cavities of different populations.

Device B shows obvious variations in deposition patterns among different demographic groups. In the group of young girls, the deposition patterns are relatively consistent, with 80% of the particles depositing in the effective area. Specifically, in CF1, 53% of the particles deposit on the nasal septum and 30% in the turbinate area, while in CF2, 44% deposit on the nasal septum and 41% in the turbinate area. Both groups have less than 10% of the particles depositing in the nasal vestibule and remaining at the outlet. In the group of young boys, the deposition proportions in the effective area vary greatly, with CM1 having about 69% deposition and CM2 having as high as 85%. However, both have a similar deposition proportion on the nasal septum, around 40%. CM2 has a 14% higher deposition in the turbinate area compared to CM1. In the adult female group, there are also clearly different. AF2 has 27% more effective deposition compared to AF1, but both have approximately 40% deposition on the nasal septum. For male adults, about 15% of the particles remain at the outlet. AM1 shows a 15% deposition in the nasal vestibule area, while AM2 has about 34%. AM1 has 19% more deposition in the effective area compared to AM2, with 53% of the deposition on the nasal septum and 17% in the turbinate area. AM2 also shows particle deposition in the olfactory area, about 8%.

The deposition distribution of Device C in the nasal cavities of different demographic groups tends to be consistent, with about 80% of particles depositing in the effective area. In this context, the deposition amount in the nasal septum area is greater than in the turbinate area, while the deposition proportion in the nasal vestibule and the residue at the outlet mostly do not exceed 10%. In the children's group, the deposition proportions in the nasal septum and turbinate areas are almost equal. In the adult group, the deposition proportion in the nasal septum area is noticeably higher than in the turbinate area. From an individual perspective, CF1 has a very high deposition proportion in the nasal septum, but the proportions in the nasal vestibule and outlet residue are both 17%, resulting in much less deposition in the turbinate area compared to others. We also found particle deposition in the olfactory area of AM2, with a deposition proportion of 13%.

Device D also shows a high degree of consistency in deposition across different demographic groups, with about 80% of particles depositing in the effective area. Among these, the deposition proportion in the nasal septum area is noticeably higher than in the turbinate area. The deposition proportion in the nasal vestibule is generally less than 10%, with the lowest being only 2%. The residue proportion at the outlet remains between 10% and 15%. In addition to AM2, which has a 10% deposition proportion in the olfactory area, we also found deposition in the olfactory area of AF1, although the deposition amount is only 3%. The adult male group has about 20% less deposition in the effective area compared to other groups, as most particles are wasted in the nasal vestibule and outlet, but the deposition in the nasal septum is almost unaffected. The 20% reduction in deposition mainly appears in the turbinate area.

3.5. Sedimentary Color Distribution

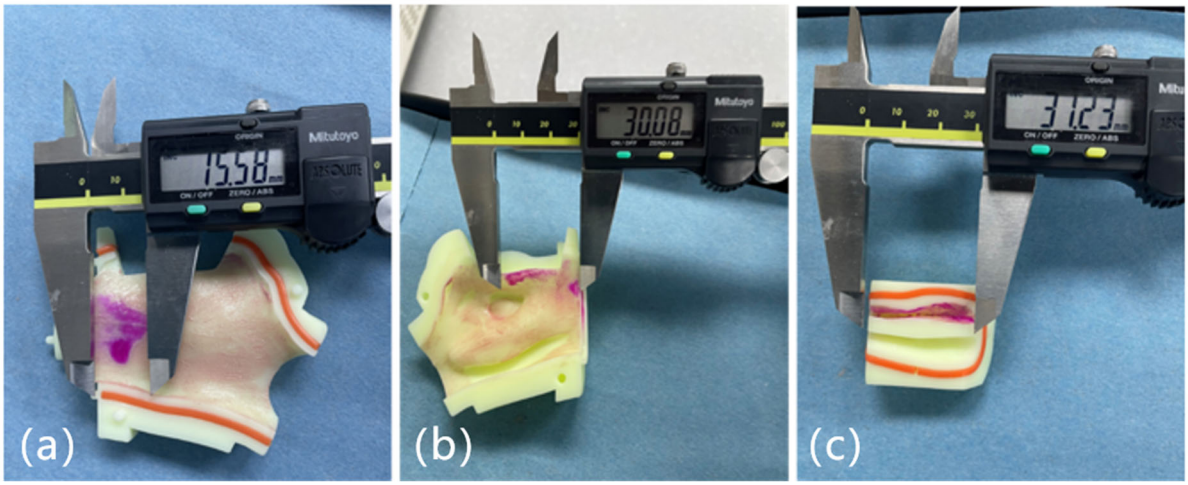

Figure 6. Depositional depth measurements of the nasal cavity, (a) septum, (b) turbinate, (c) olfactory region.

The method of color development by water test paste allows us to see the extent of the particle deposition distribution. As shown in Fig. 6, the criteria for the measurement of the deposition depth of the three regions are first introduced, and the deposition depth of both the nasal septum and the nasal turbinate are the distances between them starting from the tip of the nose until the end of the area where the particles are deposited to develop the color in the direction of the depth of the nasal cavity. For practical measurements, we divided the deposition depth of the two regions into anterior and posterior parts, the anterior part being the dimensions of the nasal vestibule, which are fixed for the same nasal cavity. The rear part is the distance from the interface between the nasal septum and the nasal vestibule to the end of the deposited developed color. The deposition depth of the olfactory region is from the anterior beginning of the olfactory region to the end of the deposition of the developed color.

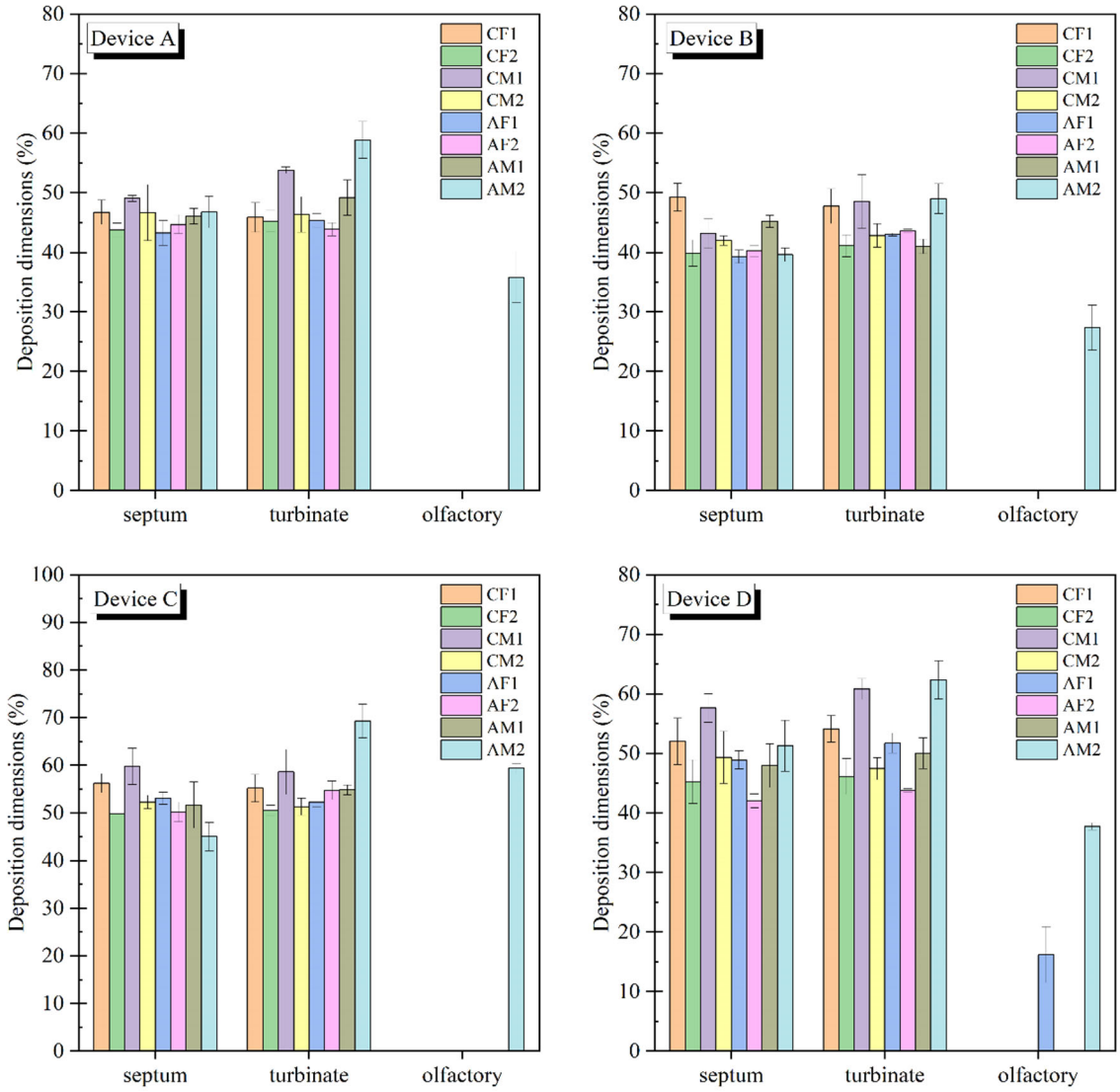

Figure 7. Deposition distribution size of the four devices in various nasal regions across different demographic groups.

As shown in Fig. 7, the deposition dimensions (the proportion of deposition depth to the length of the nasal cavity) of the four nasal sprays in the nasal cavities of different demographic groups are compared. It can be observed that the deposition depth in the nasal septum region is ordered as follows: Device B < Device A < Device D < Device C. There are also major differences between different groups. The deposition depth in the nasal septum region is noticeably smaller in the adult group compared to the children's group, and larger in the male group compared to the female group.

The deposition size patterns of the four nasal sprays in the turbinate region are generally similar to those in the nasal septum region, ordered as follows: Device B < Device A < Device D < Device C. Within the same group, the deposition depth in the turbinate region is mostly consistent among individuals, though some variations can still be observed. For example, in the male adult group, AM2 shows larger deposition depth in the turbinate region compared to AM1 for all four nasal sprays. It is also evident that the deposition depth in the male group is larger than those in the female group. In the children's group, there is no difference between the deposition depth in the turbinate and nasal septum regions. However, in the adult group, especially among males, the deposition depth in the turbinate region is better than in the nasal septum.

For the deposition depth in the olfactory area, in most cases, particles are unable to deposit in this region. Among the eight nasal cavities, only AM2 is unaffected by the nasal spray devices, with particle deposition observed in the olfactory area when using all four devices. AF1 shows particle deposition in the olfactory area only when using Device D, and the deposition depth is relatively small. Compared to the deposition depth in AM2, it can be considered negligible.

4. Discussion

Particle deposition in the nasal cavity depends on the particle size[50]. It is evident from Table IV that there is a difference in the results of particle size testing of the same nasal spray at different test points, which is consistent with findings in the literature[6]. During the atomization process, downstream droplets undergo secondary fragmentation into smaller droplets, resulting in a decrease in the average particle size[51]. The results of the study conducted by Dayal et al.

The particle size of Device D was the most stable, while the particle size of Device A varied the most with the change in test points. The particle size of Device B was much larger than that of the other three nasal sprays, almost close to twice the value. This may be related to the volume per spray of the four nasal sprays mentioned above, as the spray volume per actuation of Device B is only half that of the other nasal

sprays. In the fragmented particle morphology, the droplet size at the upstream position is noticeably larger than at the downstream position. However, the mean particle size does not change much, as the proportion of small particles in the droplet cluster is very high [52]. And the particle size in the center of the fog particle cluster is generally larger than the surrounding particle size[53]. The D10 value in this study corresponds to small particles. As the test point position changes, the number of small particles decreases, which leads to an increase in the D10 value. Therefore, as shown in Fig. 5, the proportion of deposition mass in the nasal vestibule is higher than that of the other devices, which in turn reduces the deposition in the nasal septum.

The plume angle plays a key role in the efficiency of nasal deposition[42, 54]. According to the conclusions of previous studies, the plume angle is generally 20°-40°[6, 55-58]. According to Table V, the plume angles tested in this paper ranged from 25° to 34.3°, which is in line with the conclusions of previous studies. Among them, Device C has the smallest plume angle and Device D has the largest plume angle. An increase in the plume angle will enlarge the coverage area of the particles at the same distance from the nozzle, resulting in a more uniform deposition distribution. As shown in Fig. 5, the deposition of Device D in the nasal septum and turbinate regions is relatively uniform, reducing the impact of individual differences and fluctuations. It also increases the probability of particles entering the olfactory region. The deposition results of Devices B and C show marked differences in deposition among individuals within the same region. This phenomenon may be the result of the combined effects of plume angle and individual differences. In contrast, the plume angles of Devices A and D are noticeably larger than those of Devices B and C, so their deposition results in the same region tend to be more consistent and uniform. The deposition depth in different regions of the nasal cavity is noticeably higher for Device C compared to Device B. Although both devices produce a similar plume angle, the particle size of Device C is much smaller than that of Device B. This suggests that particle size clearly influences the depth of deposition in the nasal cavity. Smaller particles are more easily delivered to the posterior regions of the nasal cavity. When the particle sizes of the devices are similar, the average deposition depth is consistent. However, an increase in plume angle causes greater fluctuations in deposition depth, as the spray pattern of the particles changes after atomization.

In order to better investigate the impact of different parameters on particle deposition within the nasal cavity, this paper will employ statistical analysis methods to explore the significance of differences in particle deposition across various regions of the nasal cavity for different individuals and devices. One-way ANOVA was used for variance analysis of continuous variables in multiple independent groups that follow a normal distribution. For multiple comparisons of means with equal variances, the Bonferroni correction was applied; for means with unequal variances, the Games-Howell correction was used. Additionally, the Kruskal-Wallis test was used for rank-sum tests of continuous variables in multiple independent groups that do not follow a normal distribution, with the Bonferroni correction applied for multiple comparisons. Table VII shows the deposition mass fractions in different regions of the nasal cavity for different individuals and devices. In the table, different lowercase letters indicate a significant difference in the deposition mass proportions in the regions of the nasal cavity for the same individual under different nasal spray devices ($P<0.05$); different uppercase letters indicate a significant difference in the deposition mass proportions in the regions of the nasal cavity for the same nasal spray device across different individuals ($P<0.05$).

From the Table VII, it can be observed that there is a significant difference in the deposition mass fraction of the nasal septum for AF2 under different devices ($p<0.05$). Device C has a higher deposition mass fraction in the nasal septum compared to Device B. There are significant differences in the deposition mass fraction of the nasal turbinate for AF1, AF2, and AM2 when using different devices. For AF1, Device D has a higher deposition mass fraction in the nasal turbinate region compared to Device B. For AF2, Device B has a higher deposition mass fraction in the nasal turbinate region compared to Device C. For AM2, the order is Device C > Device A > Device B. For the deposition mass distribution in the olfactory region, significant differences were observed between CM2 and AF1 when using different nasal spray devices. Among them, the deposition proportion of Device D was higher than the other three devices.

When controlling for the same device and considering the impact of individual differences on the deposition mass fraction, significant differences were found in the deposition mass fraction of the nasal septum between Device A and Device B. For Device A, the mass fraction of CF1 was higher than that of AM2, while for Device B, the deposition mass fraction of AM1 was higher than that of AM2. No significant differences were found for the other devices. or the differential analysis of the nasal turbinate region, significant differences were found across all four devices. For Device A, the deposition mass fraction in the nasal turbinate region follows the order: CM2 > AF2 > CF1 > CF2 > AM1 > AM2. For Device B, the order is AF2 > CM2 > CF1 > AM1 > AM2. For Device C, CM2 is higher than AF1 and AM2. For Device D, the order is CF2 > CM1 > AF1 > AF2 > AM1 > AM2. The Kruskal-Wallis test was used to examine whether there were differences in the deposition mass fraction in the olfactory region among different individuals. It was found that only Device D showed no significant difference, and that the olfactory region deposition mass fraction for AM2 was always higher than that of the other individuals. Compared to others, AM2 shows a more advantageous deposition distribution in the turbinate and olfactory regions, with more drug particles reaching deeper and farther locations. This may be related to the bilateral complete sinus window surgery it has undergone. Children, with smaller nasal cavity sizes compared to adults, are less affected by individual differences in the deposition distribution of particles within the nasal cavity during drug delivery. In contrast, due to the larger nasal cavity size in adults, individual differences have a greater impact on the deposition distribution in various regions of the nasal cavity. Under the same drug delivery conditions, the drug is more likely to reach the diseased area in the posterior nasal cavity of children, and the deposition in this region will be higher.

Table VII. Deposition mass fractions in different regions of the nasal cavity for different individuals and devices

Group	Spray device	Nasal septum (%)	Nasal turbinate (%)	Olfactory (%)
CF1	Device A	47.973±0.121aA	33.674±1.681aAB	0.000(0.000)aB
	Device B	51.446±5.237aAB	28.555±3.313aABC	0.000(0.000)aB
	Device C	44.589±5.271aA	21.551±9.422aAB	0.000(0.000)aB
	Device D	50.898±4.827aA	32.331±11.007aABC	0.000(0.000)aA
CF2	Device A	52.242±2.791aAB	33.146±2.196aAB	0.000(0.000)aB
	Device B	44.164±7.644aAB	40.568±6.856aABCD	0.000(0.000)aB
	Device C	46.704±4.657aA	39.591±5.334aAB	0.000(0.000)aB
	Device D	48.970±2.237aA	39.586±3.784aA	0.000(0.000)aA
CM1	Device A	52.696±7.476aAB	30.306±8.473aABC	0.000(0.000)aB
	Device B	35.871±7.646aAB	32.603±10.587aABCD	0.000(0.000)aB
	Device C	45.163±9.103aA	43.173±7.054aAB	0.000(0.000)aB
	Device D	40.571±5.756aA	37.756±2.337aA	0.000(0.000)aA
CM2	Device A	42.203±4.659aAB	38.773±2.684aA	0.000(0.000)bB
	Device B	42.556±5.080aAB	44.304±5.966aA	0.000(0.000)bB
	Device C	39.793±2.653aA	45.553±4.130aA	0.000(0.000)bB
	Device D	45.810±4.527aA	34.331±8.826aABC	1.620(0.486)aA
AF1	Device A	44.483±11.449aAB	33.244±6.347abAB	0.000(0.000)bB
	Device B	39.704±6.987aAB	16.339±3.890bCD	0.000(0.000)bB
	Device C	55.408±1.794aA	22.171±0.204abB	0.000(0.000)bB
	Device D	42.402±6.971aA	33.182±3.773aAB	3.143(0.859)aA
AF2	Device A	51.703±8.464abAB	35.964±7.927abA	0.000(0.000)aB
	Device B	36.228±5.019bAB	46.863±6.632aAB	0.000(0.000)aB
	Device C	56.356±3.003aA	29.784±2.857bAB	0.000(0.000)aB
	Device D	46.646±4.142abA	32.958±1.935abA	0.000(0.000)aA
AM1	Device A	50.750±4.205aAB	19.374±4.804aBC	0.000(0.000)aB
	Device B	53.009±5.880aA	16.629±1.972aBCD	0.000(0.000)aB
	Device C	51.253±10.800aA	24.530±5.867aAB	0.000(0.000)aB
	Device D	42.390±2.923aA	19.772±1.142aB	0.000(0.000)aA
AM2	Device A	41.572±1.057aB	15.229±1.897bC	9.684(1.904)aA
	Device B	34.058±4.315aB	9.181±0.070cD	8.974(1.605)aA
	Device C	42.093±8.076aA	25.121±2.022aB	13.772(2.663)aA
	Device D	38.732±1.794aA	12.274±1.326bcC	11.079(1.546)aA

5. Conclusion

This study conducted an experimental investigation of four commercial nasal sprays, using original drug formulations. Individual nasal differences, nasal spray devices, and formulation-related variables were assessed. The study investigated the effects of particle size, plume angle, and individual differences on nasal drug deposition for four commercial nasal spray devices through statistical experiments. The main conclusions are as follows:

There is a positive correlation between the size of the nasal cavity and age, and their relationship follows a linear regression equation: $y = 65.11 + 0.65x$. However, the growth rate of the olfactory region's size slows down with increasing age, and its proportion decreases.

The vast majority of particles deposit in the effective area, with the deposition order being: nasal septum > nasal turbinate > olfactory region. Additionally, most particles cannot reach the olfactory region for deposition. The deposition size distribution of nasal sprays in the nasal septum and nasal turbinate regions follows this order: Device B < Device A < Device D < Device C.

An increase in the plume angle will enlarge the coverage area of the particles at the same distance from the nozzle, resulting in a more uniform deposition distribution. The particle size clearly influences the depth of deposition in the nasal cavity. Smaller particles are more easily delivered to the posterior regions of the nasal cavity. When the particle sizes of the devices are similar, the average deposition depth is consistent. However, an increase in plume angle causes greater fluctuations in deposition depth, as the spray pattern of the particles changes after atomization.

Differences in age and gender have a major impact on the deposition distribution in the nasal septum and nasal turbinate regions, with older individuals and males exhibiting more favorable deposition patterns in these areas. This advantage becomes more pronounced with age. For patients of the same age and gender, no major differences in deposition distribution were observed in the nasal turbinate region. Compared to adults, children have smaller nasal passages, and during nasal drug administration, the deposition distribution of particles is less influenced by the patient. In contrast, in adults, due to the larger nasal passages, individual differences have a greater impact on particle deposition in various nasal regions. Under the same administration conditions, the drug is more likely to reach the posterior nasal cavity in children.

Conflict of Interest statement: The authors declare that they have no known competing financial interests or personal relationships that could have appeared to influence the work reported in this paper.

References

[1] J. Mundlia, M. Kumar, Amardeep, NASAL DRUG DELIVERY- AN OVERVIEW.

[2] B. Laube, Devices for aerosol delivery to treat sinusitis, Journal of aerosol medicine, 20 (2007) S5-S18.

[3] G. Guo, L. Zhang, T. Li, C. Li, Y. Zhang, H. Ren, Q. Zheng, Z. Tong, A. Yu, A new exhalation-assisted aerosol delivery method for nasal administration, Powder Technology, 427 (2023) 118708.

[4] L. Illum, Nasal drug delivery：possibilities, problems and solutions, J Control Release, 87 (2003) 187-198.

[5] P.G. Djupesland, A. Skretting, M. Winderen, T. Holand, Bi-directional nasal delivery of aerosols can prevent lung deposition, Journal of aerosol medicine, 17 (2003) 249-259.

[6] K. Inthavong, W. Yang, M.C. Fung, J.Y. Tu, External and Near-Nozzle Spray Characteristics of a Continuous Spray Atomized from a Nasal Spray Device, Aerosol Science and Technology, 46 (2012) 165-177.

[7] M.I. Ugwoke, R.U. Agu, N. Verbeke, R.J.A.d.d.r. Kinget, Nasal mucoadhesive drug delivery: background, applications, trends and future perspectives, 57 (2005) 1640-1665.

[8] D.-G. Yu, J.-J. Li, G.R. Williams, M. Zhao, Electrospun amorphous solid dispersions of poorly water-soluble drugs: A review, Journal of controlled release, 292 (2018) 91-110.

[9] Y. Xinchen, T. Jing, G.J.F.i.C. Jiaoqiong, Lipid-based nanoparticles via nose-to-brain delivery: A mini review, Frontiers in Cell Developmental Biology, 11 (2023) 1214450.

[10] S.A. Shah, C.J. Dickens, D.J. Ward, A.A. Banaszek, W. Horodnik, Design of experiments to optimize an in vitro cast to predict human nasal drug deposition, Journal of Aerosol Medicine Pulmonary Drug Delivery, 27 (2014) 21.

[11] P. Arora, S. Sharma, S. Garg, Permeability issues in nasal drug delivery, Drug Discovery Today, 7 (2002) 967-975.

[12] J. Chen, L. Hu, G. Yang, Q. Hu, Current therapeutic strategy in the nasal delivery of insulin: recent advances and future directions, Current Pharmaceutical Biotechnology, 19 (2018) 400-415.

[13] L.R. Hanson, W.H. Frey, Strategies for intranasal delivery of therapeutics for the prevention and treatment of neuroAIDS, Journal of Neuroimmune Pharmacology, 2 (2007) 81-86.

[14] A.R. Khan, M. Liu, M.W. Khan, G. Zhai, Progress in brain targeting drug delivery system by nasal route, Journal of Controlled Release, 268 (2017) 364-389.

[15] F. Sabir, R. Ismail, I. Csoka, Nose-to-brain delivery of antiglioblastoma drugs embedded into lipid nanocarrier systems: status quo and outlook, Drug discovery today, 25 (2020) 185-194.

[16] C. Vitorino, S. Silva, J. Bicker, A. Falcão, A. Fortuna, Antidepressants and nose-to-brain delivery: drivers, restraints, opportunities and challenges, Drug Discovery Today, 24 (2019) 1911-1923.

[17] S. Xue, X. Zhou, Z.-H. Yang, X.-K. Si, X. Sun, Stroke-induced damage on the blood–brain barrier, Frontiers in Neurology, 14 (2023) 1248970.

[18] V. Bourganis, O. Kammona, A. Alexopoulos, C. Kiparissides, Recent advances in carrier mediated nose-to-brain delivery of pharmaceutics, European Journal of Pharmaceutics Biopharmaceutics, 128 (2018) 337-362.

[19] Y.S. Kim, D.K. Sung, H. Kim, W.H. Kong, Y.E. Kim, S.K. Hahn, Nose-to-brain delivery of hyaluronate–FG loop peptide conjugate for non-invasive hypoxic-ischemic encephalopathy therapy, Journal of Controlled Release, 307 (2019) 76-89.

[20] Q. Huang, X. Chen, S. Yu, G. Gong, H. Shu, Research progress in brain-targeted nasal drug delivery, Frontiers in Aging Neuroscience, 15 (2024) 1341295.

[21] S.R. Babu, H.H. Shekara, A.K. Sahoo, P.V. Harsha Vardhan, N. Thiruppathi, M.P. Venkatesh, Intranasal nanoparticulate delivery systems for neurodegenerative disorders: A review, Therapeutic Delivery, 14 (2023) 571-594.

[22] P. Cole, The four components of the nasal valve, American journal of rhinology, 17 (2003) 107-110.

[23] X. Tong, J. Dong, Y. Shang, K. Inthavong, J. Tu, Effects of nasal drug delivery device and its orientation on sprayed particle deposition in a realistic human nasal cavity, Comput Biol Med, 77 (2016) 40-48.

[24] J.S. Kimbell, R.A. Segal, B. Asgharian, B.A. Wong, J.D. Schroeter, J.P. Southall, C.J. Dickens, G. Brace, F.J. Miller, Characterization of deposition from nasal spray devices using a computational fluid dynamics model of the human nasal passages, J Aerosol Med, 20 (2007) 59-74.

[25] J.D. Suman, B.L. Laube, R.J.P.R. Dalby, Comparison of Nasal Deposition and Clearance of Aerosol Generated by a Nebulizer and an Aqueous Spray Pump, Pharm Res, 16 (1999) 1648-1652.

[26] Kublik H, V.M. T, Nasal delivery systems and their effect on deposition and absorption, Advanced drug delivery reviews, 29 (1998) 157-177.

[27] V. Kundoor, R.N.J.P.R. Dalby, Effect of formulation- and administration-related variables on deposition pattern of nasal spray pumps evaluated using a nasal cast, Pharmaceutical Research, 28 (2011) 1895-1904.

[28] N. Sawant, M.D. Donovan, In Vitro Assessment of Spray Deposition Patterns in a Pediatric (12 Year-Old) Nasal Cavity Model, Pharm Res, 35 (2018) 108.

[29] P. Moslemi, A. Najafabadi, H. Tajerzadeh, Evaluation of different parameters that affect droplet size distribution of nasal gel sprays, Respiratory Drug Delivery, (2002) 619-622.

[30] P.G. Djupesland, Nasal drug delivery devices: characteristics and performance in a clinical perspective-a review, Drug Deliv Transl Res, 3 (2013) 42-62.

[31] Parikh, Topical corticosteroids in chronic rhinosinusitis: a randomized, double-blind, placebo-controlled trial using fluticasone propionate aqueous nasal spray, Rhinology, 39 (2001).

[32] R. Sindwani, Clinical practice guideline: adult sinusitis, Yearbook of Otolaryngology-Head Neck Surgery, 2008 (2008) 214-215.

[33] J.D.J.D.d. Suman, t. research, Current understanding of nasal morphology and physiology as a drug delivery target, Drug delivery and translational research, 3 (2013) 4-15.

[34] A. Rygg, M. Hindle, P.W.J.J.o.P.S. Longest, Linking suspension nasal spray drug deposition patterns to pharmacokinetic profiles: A proof-of-concept study using computational fluid dynamics, Journal of Pharmaceutical Sciences, 105 (2016) 1995-2004.

[35] E. Ghahramani, O. Abouali, H. Emdad, G. Ahmadi, Numerical analysis of stochastic dispersion of micro-particles in turbulent flows in a realistic model of human nasal/upper airway, Journal of aerosol science, 67 (2014) 188-206.

[36] C. Guo, W.H. Doub, The influence of actuation parameters on in vitro testing of nasal spray products, J Pharm Sci, 95 (2006) 2029-2040.

[37] M.C. Fung, K. Inthavong, W. Yang, J. Tu, CFD modeling of spray atomization for a nasal spray device, Aerosol Science and Technology, 46 (2012) 1219-1226.

[38] D.V. Doughty, L. Diao, S.W. Hoag, R.N. Dalby, Use of flexible weighted nasal spray dip tubes to improve product performance, Journal of aerosol medicine pulmonary drug delivery, 23 (2010) 69-75.

[39] P.G. Kippax, H. Krarup, J.D. Suman, Application for droplet sizing: Manual versus automated actuation of nasal sprays, (2004).

[40] F. Guidance, Bioavailability and bioequivalence studies for nasal aerosols and nasal sprays for local action, Center for Drug Evaluation Research, Rockville, MD, (2003).

[41] K. Inthavong, M.C. Fung, X. Tong, W. Yang, J. Tu, High resolution visualization and analysis of nasal spray drug delivery, Pharm Res, 31 (2014) 1930-1937.

[42] M.Y. Foo, Y.S. Cheng, W.C. Su, M.D. Donovan, The influence of spray properties on intranasal deposition, J Aerosol Med, 20 (2007) 495-508.

[43] C. Guo, K.J. Stine, J.F. Kauffman, W.H. Doub, Assessment of the influence factors on in vitro testing of nasal sprays using Box-Behnken experimental design, Eur J Pharm Sci, 35 (2008) 417-426.

[44] Y.S. Cheng, T.D. Holmes, J. Gao, R.A. Guilmette, S. Li, Y. Surakitbanharn, C. Rowlings, Characterization of nasal spray pumps and deposition pattern in a replica of the human nasal airway, J Aerosol Med, 14 (2001) 267-280.

[45] L. Golshahi, M.L. Noga, R.B. Thompson, W.H. Finlay, In vitro deposition measurement of inhaled micrometer-sized particles in extrathoracic airways of children and adolescents during nose breathing, Journal of Aerosol Science, 42 (2011) 474-488.

[46] P.G. Djupesland, A. Skretting, M. Winderen, T. Holand, Breath actuated device improves delivery to target sites beyond the nasal valve, The Laryngoscope, 116 (2006) 466-472.

[47] K. Inthavong, Q. Ge, C.M.K. Se, W. Yang, J.Y. Tu, Simulation of sprayed particle deposition in a human nasal cavity including a nasal spray device, Journal of Aerosol Science, 42 (2011) 100-113.

[48] K. Inthavong, W. Yang, M.C. Fung, X.W. Tong, J.Y. Tu, Spray Characteristics and Droplet Size Distributions From Low Pressure Spray Atomisation, Proceedings of the 19th Australasian Fluid Mechanics Conference 2014 Australasian Fluid Mechanics Society (AFMS 2014), (2014) 1-4.

[49] S.H. MD Manniello, A Alfaifi, AR Esmaeili, AV Kolanjiyil, R Walenga, A Babiskin, In vitro evaluation of regional nasal drug delivery using multiple anatomical nasal replicas of adult human subjects and two nasal sprays, International Journal of Pharmaceutics, 593 (2021) 120103.

[50] R. Dahl, Mygind, N., Anatomy, physiology and function of the nasal cavities in health and disease, Advanced Drug Delivery Reviews, 29 (1998) 3-12.

[51] P.D.M.S.S.M. Singh, Evaluation of different parameters that affect droplet-size distribution from nasal sprays using the Malvern Spraytec, 93(7) (2004) 1725–1742.

[52] K.Y. Inthavong, W.; Fung, M. C.; Tu, J. Y, External and Near-Nozzle Spray Characteristics of a Continuous Spray Atomized from a Nasal Spray Device, Aerosol Science and Technology, 46(2) (2012) 165–177.

[53] J.Z. Lin, T.L. Chan, S. Liu, K. Zhou, Y. Zhou, S.C. Lee, Effects of Coherent Structures on Nanoparticle Coagulation and Dispersion in a Round Jet, J International Journal of Nonlinear Sciences Numerical Simulation, 8 (2007) 45-54.

[54] Y.S.H. Cheng, T.D.; Gao, J.; Guilmette, R.A.; Li, S.; Surakitbanharn, Y.; Rowlings, C, Characterization of Nasal Spray Pumps and Deposition Pattern in a Replica of the Human Nasal Airway, Journal of Aerosol Medicine, 14(2) (2001) 267–280.

[55] J. Siu, K. Shrestha, K. Inthavong, Y. Shang, R. Douglas, Particle deposition in the paranasal sinuses following endoscopic sinus surgery, Computers in Biology and Medicine, 116 (2020) 103573.

[56] K.F. Inthavong, Man Chiu; Tong, Xuwen; Yang, William; Tu, Jiyuan High Resolution Visualization and Analysis of Nasal Spray Drug Delivery, Pharmaceutical Research, 31(8) (2014) 31(38), 1930–1937.

[57] K. Inthavong, M.C. Fung, W. Yang, J. Tu, Measurements of droplet size distribution and analysis of nasal spray atomization from different actuation pressure, J Aerosol Med Pulm Drug Deliv, 28 (2015) 59-67.

[58] M.C. Fung, K. Inthavong, W. Yang, P. Lappas, J. Tu, External characteristics of unsteady spray atomization from a nasal spray device, J Pharm Sci, 102 (2013) 1024-1035.